

# The effects of parametric uncertainties on the nonlinear vibrations of a pressure-loaded spherical hyperelastic membrane

Kaio. C. B. Benedetti<sup>1,a</sup>, Frederico M. A. da Silva<sup>2,b</sup>, Renata M. Soares<sup>2,c</sup>, Paulo B. Gonçalves<sup>1,d</sup>

<sup>1</sup>*Dept. of Civil and Environmental Engineering, Pontifical Catholic University of Rio de Janeiro  
R. Marquês de São Vicente, 225, Gávea, 22451-900, Rio de Janeiro/RJ, Brazil*

<sup>a</sup>*kaio.engcivil@aluno.puc-rio.br*, <sup>d</sup>*paulo@puc-rio.br*

<sup>2</sup>*School of Civil and Environmental Engineering, Federal University of Goiás*

*Av. Universitária, Quadra 86, Lote Área 1488, Setor Leste Universitário, 74605-220, Goiânia/GO, Brazil*

<sup>b</sup>*silvafma@ufg.br*, <sup>c</sup>*renatasoares@ufg.br*

**Abstract.** Hyperelastic membranes are found in many engineering fields. A key step in their mathematical modelling is the choice of an appropriate constitutive law and, subsequently, the determination of the associated material parameters, usually obtained from experimental results, with the occurrence of multiple sets of optimal material parameters for the same data sets, depending on the fitting process. The influence of the constitutive law of a hyperelastic material on its nonlinear behavior is well known and both static and dynamic responses can vary greatly, depending on the parameter values. Thus, the application of the uncertainty propagation analysis, capturing the expected outcome in a probabilistic sense, constitutes an interesting tool in the analysis of hyperelastic structures, particularly in the dynamic case. Here it is applied to the analysis of a pressure-loaded spherical hyperelastic membrane with constitutive uncertainty. Different hyperelastic constitutive models are addressed, comparing the static and dynamic nonlinear response under parametric uncertainty. Finally, the global stability is developed by expanding a previous concept of  $(Q, \Lambda)$ -attractors to the dual space where basins are defined. Specifically, the inclusion of parametric uncertainty is responsible for the diffusion of attractors and basins boundaries, drastically changing the phase-space topology. A novel methodology of phase-space discretization is also considered to represent the phase-space topology under uncertainty. A global dynamical analysis framework in the context of parametric uncertainty is yet to be addressed, specifically for hyperelastic constitutive models, constituting the novelty of the present work.

**Keywords:** Parametric uncertainties, hyperelastic material, constitutive models, spherical membrane, global dynamics.

## 1 Introduction

The applicability of spherical membranes is vast, being found in many engineering fields, such as spatial structures, containers, and deployable structures, see Jenkins [1]. Furthermore, they can undergo large displacements in the operational stage, requiring nonlinear mechanics to be modelled for the correct representation of the physical system.

However, there are many possible material models to represent hyperelastic materials. Depending on this choice, the nonlinear effects can be drastically different, see Silva et al. [2]. For the case of spherical membranes, specifically, there can be one or two potential wells, with unbounded solutions for the first case. Furthermore, complicate nonlinear behavior is observed for the dynamically excited membrane. Even if a material model is defined, usually it depends on various parameters, which are difficult to define experimentally, as demonstrated by Ogden et al. [3].

This parametric uncertainty has been explored in recent years, under the alias of stochastic hyperelastic constitutive laws. Staber and Guilleminot derived models for general incompressible hyperelastic materials [4]

and for compressible Odgen type materials [5]. They pointed essential conditions that the energy function must satisfy for the response to be meaningful, namely, that they are polyconvex and coherent at small strains. Later, those concepts were reformulated by Mihai and coworkers [6–8] as material objectivity, material isotropy, Baker-Ericksen inequalities, and, for the stochastic case, finite mean and variance of the random shear modulus. Such conditions implies that the Odgen material parameters that composes the shear modulus must all be finite and positive, and if uncertainty is assumed, the distribution is of gamma type according to the maximum entropy principle. However, the influence of such uncertainties in the nonlinear dynamics is still being explored, with limited progress regarding global dynamics.

This work concentrates in the analysis of hyperelastic spherical membrane with Odgen type material. The model will be taken from a previous work [2], namely an Odgen model with 3 terms, and parametric uncertainty with gamma distribution is assumed. The global dynamics of this system is explored, demonstrating the effect of uncertainty over both the attractors' distributions and basins of attraction. The transfer operator framework is adapted from Dellnitz et al. [9], substituting the Monte Carlo by a stochastic collocation via Laguerre-chaos, see Xiu and Karniadakis [10], thus diminishing the computational cost of the analysis.

## 2 Hyperelastic membrane formulation

The physical problem consists of a closed, homogeneous, isotropic and hyperelastic spherical membrane of initial radius  $a$ , thickness  $h$  and density  $\gamma$ . It is assumed that  $h/a \ll 1$ , therefore the theory of thin-walled membranes under finite deformations can be considered. The formulation for axisymmetric motions was previously developed by Silva et al. [2], assuming materials of neo-Hookean and Odgen type. Adopting the stretch ratio  $x = A/a$ , where  $A$  is the deformed radius, the full nondimensional equation of movement for the general Odgen material is

$$\ddot{x} + f(x)\dot{x} + \sum_{i=1}^N \frac{\mu_i}{\mu_1} \left[ (x + x_s)^{\alpha_i-1} - (x + x_s)^{-2\alpha_i-1} \right] = Q_s (x + x_s)^2 [1 + \beta \cos(\Omega \tau)], \quad (1)$$

where  $N$  is the number of terms,  $\mu_i$  and  $\alpha_i$  are the material constants,  $f(x)$  is the damping function. A static component takes part in the equation,  $x_s$ , resulted from the static preload  $Q_s$ . A harmonic perturbation of the static equilibrium is defined, with amplitude ratio  $\beta$  and frequency  $\Omega$ . The nondimensional time variable is  $\tau = t(2\mu_1/\gamma a^2)^{1/2}$ , and  $\dot{x} = dx/d\tau$ . Finally, the damping function is defined as [2]

$$f(x) = 2\omega_0 \zeta + \xi x^2, \quad (2)$$

where  $\zeta$  and  $\xi$  are the linear and cubic nondimensional damping coefficients.

The static variables must be calculated before eq. (1) takes place. Specifically, the static displacement is obtained from eq. (1) by setting the time dependent variables to zero, resulting in

$$\sum_{i=1}^N \frac{\mu_i}{\mu_1} (x_s^{\alpha_i-3} - x_s^{-2\alpha_i-3}) = Q_s. \quad (3)$$

The lowest natural frequency can also be obtained from eq. (1). By linearizing it around the static equilibrium and setting to zero the damping function, we obtain

$$\ddot{x} + \left\{ \sum_{i=1}^N \frac{\mu_i}{\mu_1} [(\alpha_i - 3)x_s^{\alpha_i-2} + (2\alpha_i + 3)x_s^{-2\alpha_i-2}] \right\} x = 0, \quad (4)$$

and, by inspection, the nondimensional natural frequency is

$$\omega_0^2 = \sum_{i=1}^N \frac{\mu_i}{\mu_1} [(\alpha_i - 3)x_s^{\alpha_i-2} + (2\alpha_i + 3)x_s^{-2\alpha_i-2}], \quad (5)$$

coinciding with the development of Gonçalves [11].

The analysis follows from a static position, obtained from eq. (3) given a preload  $Q_s$ . The natural frequency is then calculated by eq. (5), and thus the damping force is defined, eq. (2). The equation of movement can them

be applied, eq. (1), describing the nonlinear breathing motions of the hyperelastic membrane.

One of the material parameters is adopted as uncertain. However, important aspects must be considered so that eq. (1) can adequately represent the physical problem. The developments of Staber and Guillemot [4] identified that the parameters  $\mu_i$  must have a gamma distribution if uncertainty is assumed. Therefore, uncertainty in  $\mu_i$  will be represented as an additive component,  $\lambda$ , with distribution

$$p(\lambda; \alpha) = \frac{e^{-\lambda} \lambda^\alpha}{\Gamma(1+\alpha)}, \quad 0 \leq \lambda < \infty, \alpha > -1 \quad (6)$$

with mean  $\bar{\lambda} = \alpha + 1$  and variance  $\sigma_\lambda^2 = \alpha + 1$ , see Xiu and Karniadakis [10].

### 3 Global dynamics under parametric uncertainty

The effect of parametric uncertainty can be observed over the attractors' densities of eq. (1). Dellnitz et al. [9] developed the  $(Q, \Lambda)$ -Attractor concept to account for parametric uncertainty. This is achieved through global dynamic analysis, expanding the original Ulam method. Given the flow map  $\varphi(x, \lambda)$  generated by the dynamical system with uncertainty parameter  $\lambda$ , and a cellular subdivision  $\{b_1, \dots, b_n\}$  of the phase-space, each entry of the transfer matrix is computed by Dellnitz et al. [9] as

$$p_{ij} = \frac{m(\varphi^{-1}(b_i, \lambda) \cap b_j)}{m(b_j)} \approx \frac{1}{n_b n_\lambda} \sum_{k=1}^{n_i} \{l \in \{1, \dots, n_b\} | \varphi(x_l, \lambda_k) \in b_j\}, \quad (7)$$

where  $m(\alpha)$  is the measure of  $\alpha$ . Therefore, a Monte Carlo approach is conducted, sampling  $n_b$  points in each cell  $b_i$  with  $n_\lambda$  parameter values randomly selected of the probability distribution of  $\lambda$ . Each  $p_{ij}$  entry is then the mean flux over the probability space spanned by the uncertainty. This same approach can be extended for stochastic dynamic systems by identifying the sample-path probability space, as previously done by Benedetti and Gonçalves [12].

The Monte Carlo approach is, nevertheless, computationally expensive. To alleviate this, we recede to the continuous definition of the transfer matrix, i. e., the Perron-Frobenius operator and the Foias operator, see Lasota and Mackey [13]. It is defined as

$$\mathcal{F}_i \int_B f dx = \int_{\mathbb{X}} \left\{ \int_{\Lambda} \text{id}_B [\varphi_t(\lambda, x)] P(d\lambda) \right\} f dx, \quad (8)$$

and its discretization due to the cellular subdivision of the phase-space is

$$p_{ij} = \frac{1}{m(b_i)} \int_{b_i} \left\{ \int_{\Lambda_x(b_j)} P(d\lambda) \right\} dx. \quad (9)$$

As we can check in eq. (9), the Monte Carlo approach of eq. (7) approximates the integrals over the phase-space and probability space. Here, we conducted a stochastic collocation approach, substituting the integral over the probability space by a weighted sum. Specifically for gamma distributions, the Laguerre-Chaos polynomials are employed. For more details regarding the stochastic collocation procedure, we refer to Xiu and Karniadakis [10].

### 4 Results

For this analysis we considered a parameter set from Odgen et al. [3], which were also analyzed by Silva et al. [2], namely the OSS2 model with  $N = 3$ . They are resumed in Table 1. The damping, static preload and dynamic amplitude and frequency are also from [2]. They are resumed in Table 2. Finally, the parametric uncertainty case aborded in this work is defined by adding a gamma variable  $\lambda$  to the first shear parameter,  $\mu_1$ .

Table 1. Material parameters of model OSS2

$I$	$\alpha_i$	$\mu_i$
1	1.6918	4.4184
2	5.4929	0.013381
3	1.6919	0.47456

The global dynamic analysis was conducted over the phase-space window  $[-0.9;9] \times [-12;12]$ . The cellular partition was constructed incrementally, from 32 divisions per dimension up to 256 division per dimension, flagging the basin boundaries and attractors' densities. Also, the number of initial conditions in each cell is a function of the cell size, starting at 144 points and ending at 36 points. For the uncertainty parameter, we adopted five points in the probability space to compound the stochastic collocation, so that each point was integrated five times, with 5 different parameter values, for 1-period of excitation. Finally, the classical fourth order Runge-Kutta was adopted, with time step  $\Delta\tau = 2\pi/2000\Omega$ .

Table 2 Static preload, damping and forcing terms

parameters	value
$x_s$	1.030073206696912
$Q_s$	0.15
$\zeta$	0.01
$\tilde{\zeta}$	0.01
$\beta$	0.8
$\Omega$	2.1514

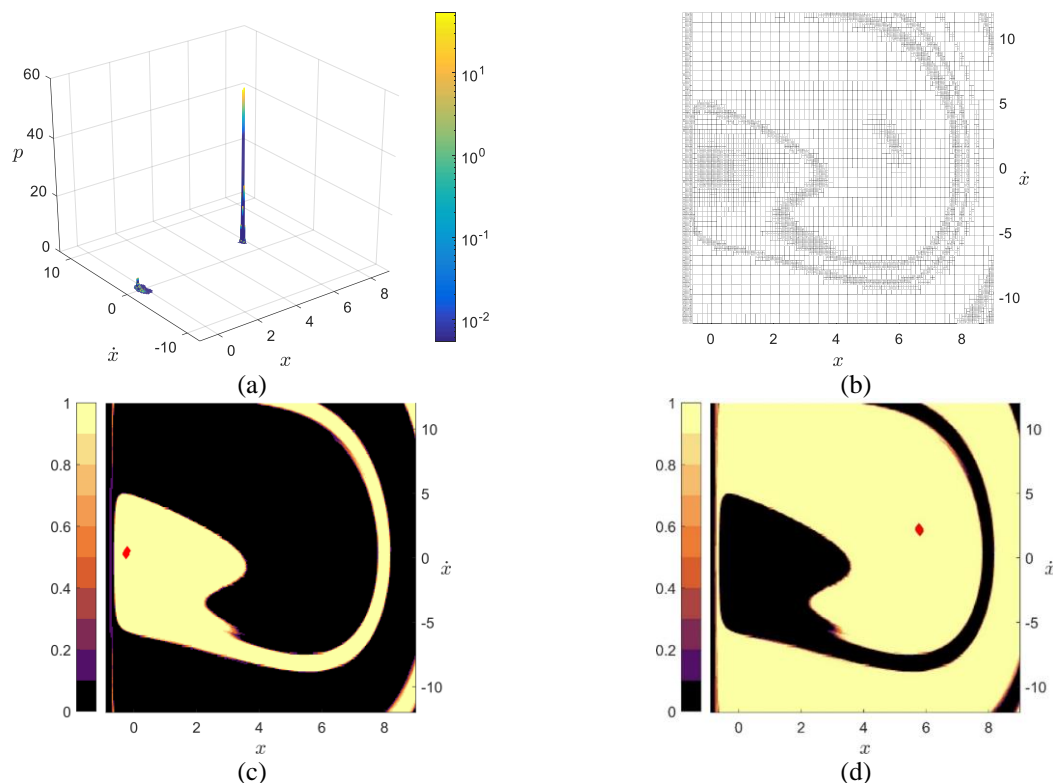


Figure 1. Global dynamics of the deterministic case: (a) attractors' densities, (b) phase-space final subdivision, (c) nonresonant basin of attraction, (d) resonant basin of attraction

The first analysis consists of deterministic results. The densities are presented in Fig. 1a, where two attractors are clearly depicted, one of small amplitude (nonresonant) and other with large amplitude (resonant). The resonant attractor shows a higher density, which indicates that it has the larger basin of attraction. This is confirmed by inspection of the basin of attractions, presented in Figs. 1c, d. In the basins, the attractors are depicted as red markings, since Dirac delta distributions are expected in the deterministic case. The final phase-space subdivision is depicted in Fig. 1b, showing the capability of the methodology to locally refine the basins boundaries and attractors' densities. The subdivision procedure was expanded upon the global dynamics' algorithms used in GAIO, by Dellnitz and coworkers [14].

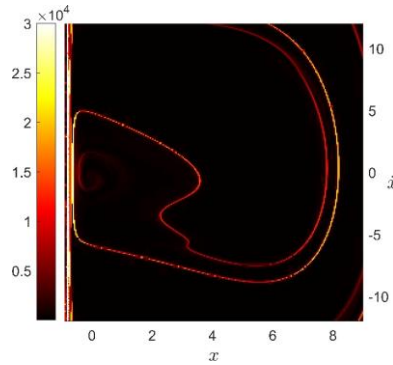


Figure 2. Lagrangian descriptor gradient

Figure 2 contains the gradient of the lagrangian descriptor (LD). This is an additional result, calculated following Beneitez et al. [15], which marks the basins boundaries. As expected, the phase-space is more refined where the LC gradient has high values.

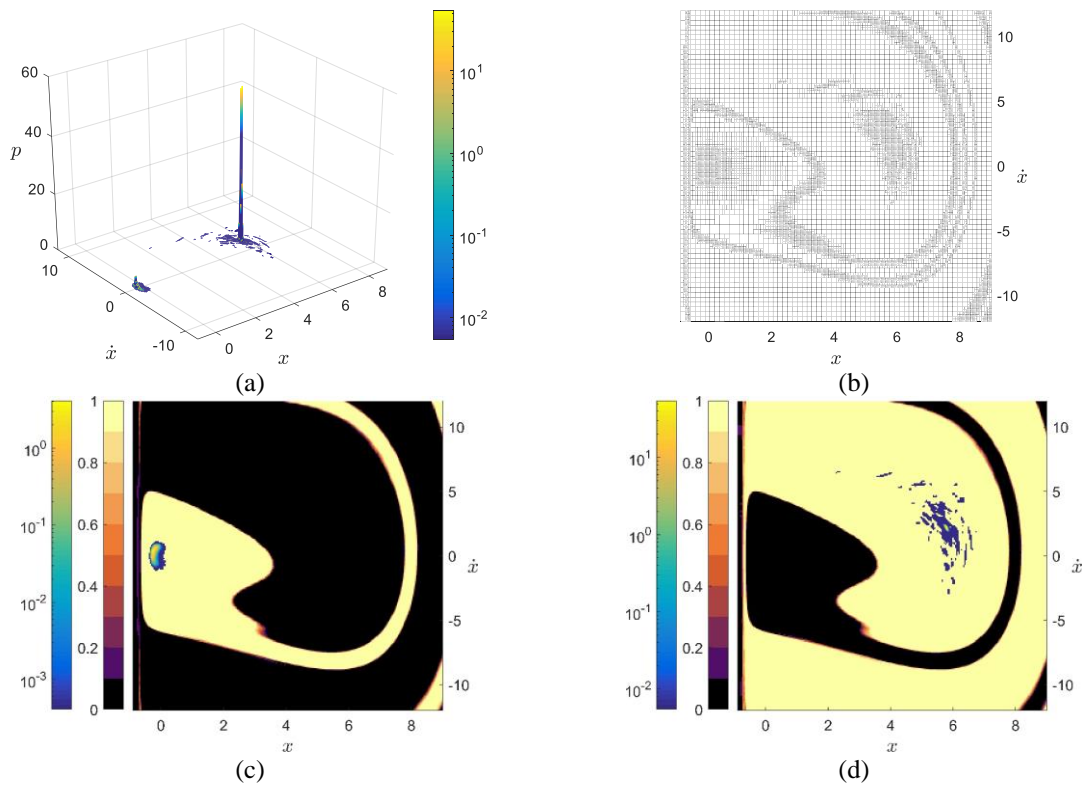


Figure 3. Global dynamics of parametric uncertainty case with  $\alpha = -0.9999$ : (a) attractors' densities, (b) phase-space final subdivision, (c) nonresonant basin of attraction, (d) resonant basin of attraction

The next result is the first with parametric uncertainty, with  $\alpha = -0.9999$ , Fig. 3. The uncertainty effect is more present in the attractors' densities, Fig. 3a, specifically in the resonant attractor, spreading it over the phase-space. This is more noticeable also in the phase-space subdivision, Fig. 3b, where this attractor is more refined. The basins of attraction display almost no difference with respect to the deterministic case, Fig. 3c, d. It is surprising that such a small random perturbation could change one density to this degree, but its basin remains still.

Lastly, the second parametric uncertainty case with  $\alpha = -0.99$  is presented in Fig. 4. The resonant attractor is heavily affected by the uncertainty, spreading over a large area of the phase-space, Fig. 4a. This is more detailed in the phase-space subdivision, Fig. 4b, where the resonant attractor region is increasingly refined. The basins of attraction, Figs. 4c, d, are surprisingly insensitive to this uncertainty level, with boundaries remained localized in the phase-space. However, the overlapping attractor of the resonant case reveals that its density is close to the boundary, Fig. 4d, meaning that any perturbation could drastically change the global dynamics. This is confirmed when we tried to verify the case for  $\alpha > -0.99$ , where the resonant attractor is destroyed.

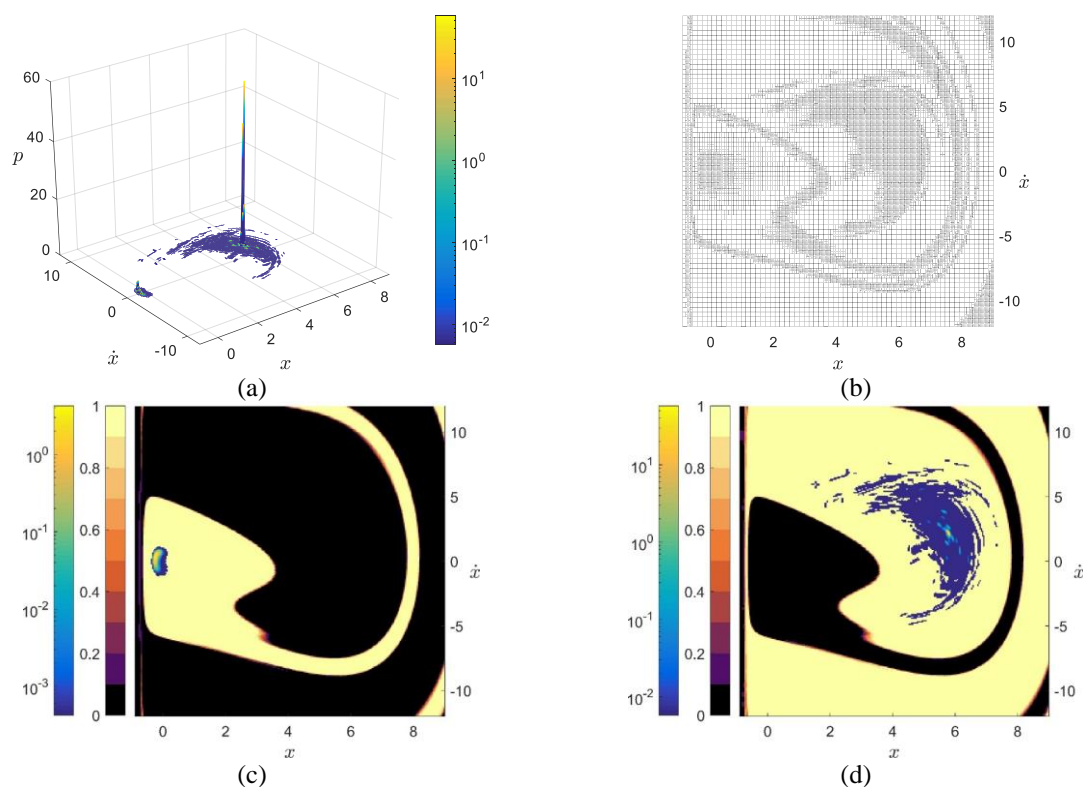


Figure 4. Global dynamics of parametric uncertainty case with  $\alpha = -0.99$ : (a) attractors' densities, (b) phase-space final subdivision, (c) nonresonant basin of attraction, (d) resonant basin of attraction

## 5 Conclusions

The effects of parametric uncertainty on the global dynamics of a hyperelastic spherical membrane was addressed. An Odgen material type with three terms was considered with uncertainty in the first component of the shear modulus. The computational cost of the analysis was alleviated by considering stochastic collocation to obtain the mean transfer matrix and, consequently, the mean results. The mean results demonstrate the sensitivity of the model in the parameter values, where the resonant response was destroyed in the mean sense for just a small parametric perturbation. Other parametric uncertainty cases and their effects over nonlinear and global dynamics will be investigated in a future research.

**Acknowledgements.** The authors acknowledge the financial support of the Brazilian research agencies CAPES [finance code 001], CNPq, FAPERJ-CNE and FAPERJ Nota 10

**Authorship statement.** The authors hereby confirm that they are the sole liable persons responsible for the authorship of this work, and that all material that has been herein included as part of the present paper is either the property (and authorship) of the authors, or has the permission of the owners to be included here.

## References

- [1] C. H. M. Jenkins, *Gossamer Spacecraft: Membrane And Inflatable Structures Technology For Space Applications*. American Institute of Aeronautics and Astronautics, Reston ,VA, 2001.
- [2] F. M. A. da Silva, R. M. Soares, Z. J. G. N. Del Prado, and P. B. Gonçalves, "Intra-well and cross-well chaos in membranes and shells liable to buckling". *Nonlinear Dyn*, vol. 102, n. 2, pp. 877–906, 2020.
- [3] R. W. Ogden, G. Saccomandi, and I. Sgura, "Fitting hyperelastic models to experimental data". *Comput Mech*, vol. 34, n. 6, pp. 484–502, 2004.
- [4] B. Staber and J. Guilleminot, "Stochastic modeling of a class of stored energy functions for incompressible hyperelastic materials with uncertainties". *Comptes Rendus Mécanique*, vol. 343, n. 9, pp. 503–514, 2015.
- [5] B. Staber and J. Guilleminot, "Stochastic modeling of the Ogden class of stored energy functions for hyperelastic materials: the compressible case". *ZAMM - J Appl Math Mech / Zeitschrift für Angew Math und Mech*, vol. 97, n. 3, pp. 273–295, 2017.
- [6] L. A. Mihai, D. Fitt, T. E. Woolley, and A. Goriely, "Likely equilibria of stochastic hyperelastic spherical shells and tubes". *Math Mech Solids*, pp. 108128651881188, 2018.
- [7] L. A. Mihai, D. Fitt, T. E. Woolley, and A. Goriely, "Likely oscillatory motions of stochastic hyperelastic solids". *Trans Math Its Appl*, vol. 3, n. 1, 2019.
- [8] L. A. Mihai, T. E. Woolley, and A. Goriely, "Likely cavitation and radial motion of stochastic elastic spheres". *Nonlinearity*, vol. 33, n. 5, pp. 1987–2034, 2020.
- [9] M. Dellnitz, S. Klus, and A. Ziessler, "A Set-Oriented Numerical Approach for Dynamical Systems with Parameter Uncertainty". *SIAM J Appl Dyn Syst*, vol. 16, n. 1, pp. 120–138, 2017.
- [10] D. Xiu and G. E. Karniadakis, "The Wiener-Askey Polynomial Chaos for Stochastic Differential Equations". *SIAM J Sci Comput*, vol. 24, n. 2, pp. 619–644, 2002.
- [11] P. B. Gonçalves, "Axisymmetric Vibrations of Imperfect Shallow Spherical Caps Under Pressure Loading". *J Sound Vib*, vol. 174, n. 2, pp. 249–260, 1994.
- [12] K. C. B. Benedetti and P. B. Gonçalves, "Nonlinear response of an imperfect microcantilever static and dynamically actuated considering uncertainties and noise". *Nonlinear Dyn*, vol. 2, 2021.
- [13] A. Lasota and M. C. Mackey, *Chaos, Fractals, and Noise*, 2nd ed. Springer New York, New York, NY, 1994.
- [14] M. Dellnitz, A. Hohmann, O. Junge, and M. Rumpf, "Exploring invariant sets and invariant measures". *Chaos An Interdiscip J Nonlinear Sci*, vol. 7, n. 2, pp. 221–228, 1997.
- [15] M. Beneitez, Y. Duguet, P. Schlatter, and D. S. Henningson, "Edge manifold as a Lagrangian coherent structure in a high-dimensional state space". *Phys Rev Res*, vol. 2, n. 3, pp. 033258, 2020.